Rhodium Phosphines Partnered with the Carborane Monoanions $[CB_{11}H_6Y_6]^-$ (Y = H, Br). Synthesis and Evaluation as Alkene Hydrogenation Catalysts

Adem Rifat, Nathan J. Patmore, Mary F. Mahon, and Andrew S. Weller*

Department of Chemistry, University of Bath, Bath BA2 7AY, U.K.

Received January 31, 2002

Addition of Ag[*closo*-$CB_{11}H_{12}$] to $[(PPh_3)_2RhCl]_2$ affords the new *exo*polyhedrally coordinated complex $[(PPh_3)_2Rh(closo\text{-}CB_{11}H_{12})]$ (**1**), which has been characterized by multinuclear NMR spectroscopy and X-ray crystallography. Using the less nucleophilic [*closo*-$CB_{11}H_6Br_6]^-$ anion afforded the arene-bridged dimer $[(PPh_3)(PPh_2\text{-}\eta^6\text{-}C_6H_5)Rh]_2[closo\text{-}CB_{11}H_6Br_6]_2$ (**2**) with poor compositional purity. However, with the new precursor complexes $[(PPh_3)_2Rh(nbd)][Y]$ (Y = *closo*-$CB_{11}H_{12}$ (**3**), *closo*-$CB_{11}H_6Br_6$ (**4**); nbd = norbornadiene) as starting materials, treatment with H_2 affords **1** and **2** in good yield and compositional purity. Complex **2** has been characterized by multinuclear NMR spectroscopy and X-ray diffraction. The new complexes **3** and **4** have been evaluated as internal alkene hydrogenation catalysts using the substrates cyclohexene, 1-methylcyclohexene, and 2,3-dimethylbut-2-ene under the attractive conditions of room temperature and pressure. These new catalysts have also been compared with $[(PPh_3)_2Rh(nbd)][BF_4]$ and Crabtree's catalyst, $[(py)(PCy_3)Ir(cod)][PF_6]$ (cod = 1,5-cyclooctadiene). A clear counterion effect is observed. For the hydrogenation of cyclohexene the $[BF_4]^-$ and [*closo*-$CB_{11}H_{12}]^-$ salts are broadly similar, but the [*closo*-$CB_{11}H_6Br_6]^-$ salt is significantly better, matching Crabtree's catalyst in hydrogenation efficiency. This pattern is mirrored in the hydrogenation of 1-methylcyclohexene and the sterically hindered 2,3-dimethylbut-2-ene, although with the latter substrate Crabtree's catalyst does outperform **4**. Nevertheless, these results are excellent for a rhodium complex, which have traditionally been considered as ineffectual catalysts for the hydrogenation of internal alkenes at room temperature and pressure. The deactivation product in the catalytic cycle, $[(PPh_3)_2HRh(\mu\text{-}Cl)_2(\mu\text{-}H)RhH(PPh_3)_2][CB_{11}H_{12}]$ (**5**), has been characterized by multinuclear NMR spectroscopy and X-ray crystallography.

Introduction

The use of rhodium-based catalysts of the general types $RhCl(PR_3)_3$ and $[(PR_3)_2Rh(nbd)]^+$ (nbd = norbornadiene) for the hydrogenation of olefins has been a topic of significant academic and commercial interest over the last 30 years.[1−4] However, one limitation of these systems is that they are relatively slow for the hydrogenation of internal double bonds under ambient laboratory conditions.[5,6] This methodological gap is, in part, filled by iridium-based catalysts, such as [(cod)Ir(pyridine)PCy_3][PF_6] (cod = 1,5-cyclooctadiene)[5,7,8] or related compounds,[9] which are significantly better at the room-temperature and -pressure hydrogenation of sterically demanding internal alkenes than their rhodium counterparts $[(PPh_3)_2Rh(nbd)][PF_6]$ and $RhCl(PPh_3)_3$. Since the catalysts of choice for hydrogenation of an alkene are often based around cationic metal fragments, such as $\{(L)_2Rh(diene)\}^+$ and $\{(L)_2Ir(diene)\}^+$ (L = phosphine), it is always necessary to pair these with an anionic counterion such as $[BF_4]^-$ or $[PF_6]^-$. The role of the counterion in metal-mediated catalysis in general is becoming increasingly appreciated,[10−12] and as far as hydrogenation reactions are concerned, notable examples exist of increases in both overall efficiency and enantioselectvity on changing the counterion.[13−16] Central to the work reported here is the use of *least*

* To whom correspondence should be addressed. Tel: (01225) 323394. Fax: (01225) 826231. E-mail: a.s.weller@bath.ac.uk.

(1) Brunner, H. Hydrogenation. In *Applied Homogeneous Catalysis with Organometallic Compounds*; Cornils, B., Hermann, W. A., Eds.; Wiley-VCH: Weinheim, Germany, 2000; p 201.
(2) Schrock, R. R.; Osborn, J. A. *J. Am. Chem. Soc.* **1976**, *98*, 2134.
(3) Noyori, R. *Asymmetric Catalysis in Organic Synthesis*; Wiley: New York, 1994.
(4) Gridnev, I. D.; Yasutake, M.; Higashi, N.; Imamoto, T. *J. Am. Chem. Soc.* **2001**, *123*, 5268.
(5) Crabtree, R.; Gautier, A.; Giordano, G.; Khan, T. *J. Organomet. Chem.* **1977**, *141*, 113.
(6) Parshall, G. W.; Ittel, S. D. *Homogeneous Catalysis*, 2nd ed.; Wiley: New York, 1992.
(7) Crabtree, R. *Acc. Chem. Res.* **1979**, *12*, 331.
(8) Crabtree, R.; Demou, P. C.; Eden, D.; Mihelcic, J. M.; Parnell, C. A.; Quirk, J. M.; Morries, G. E. *J. Am. Chem. Soc.* **1982**, *104*, 6994.
(9) Lee, H. M.; Jiang, T.; Stevens, E. D.; Nolan, S. P. *Organometallics* **2001**, *20*, 1255.
(10) Evans, D. A.; Lectka, T.; Matt, P. V.; Miller, S. J. *J. Am. Chem. Soc.* **1999**, *121*, 7559.
(11) Kündig, E. P.; Saudan, C. M.; Bernardinelli, G. *Angew. Chem., Int. Ed.* **1999**, *38*, 1220.
(12) Chen, E. Y. X.; Marks, T. J. *Chem. Rev.* **2000**, *100*, 1391.
(13) Ohta, T.; Ikegami, H.; Miyake, T.; Takaya, H. *J. Organomet. Chem.* **1995**, *502*, 169.
(14) Buriak, J. M.; Osborn, J. A. *Organometallics* **1996**, *15*, 3161.
(15) (a) Lightfoot, A.; Schinder, O.; Pfaltz, A. *Angew. Chem., Int. Ed.* **1998**, *37*, 2897. (b) Blackmond, D. G.; Lightfoot, A.; Pflatz, A.; Rosner, T.; Schnider, P.; Zimmermann, N. *Chirality* **2000**, *12*, 442.
(16) Buriak, J. M.; Klein, J. C.; Herrington, D. G.; Osborn, J. A. *Chem. Eur. J.* **2000**, *6*, 139.

10.1021/om020077r CCC: $22.00
Publication on Web 06/04/2002

coordinating anions[17] to increase reaction rates and yields of product in catalytic processes that implicate a cationic, unsaturated metal center. We have a current interest in the use of weakly coordinating carborane monoanions[18] partnered with Lewis acidic metal/ligand fragments,[19−21] and have recently demonstrated that significant gains in rate enhancement and catalyst stability can be brought about by using anions derived from [*closo*-$CB_{11}H_{12}]^-$ in a silver(I) phosphine catalyzed hetero Diels−Alder reaction.[22] In particular, the use of the hexabromo-substituted carborane [*closo*-$CB_{11}H_6Br_6]^-$ affords a catalyst that shows significant increases in observed rate for this reaction over [*closo*-$CB_{11}H_{12}]^-$ and other, more conventional counterions such as perchlorate and tetrafluoroborate.

Metallacarboranes, and especially rhodacarboranes, have been shown to be active homogeneous catalysts for alkene hydrogenation. This was first demonstrated by Hawthorne,[23−28] who also elucidated the mechanistic aspects of these catalysts,[29] showing that an *exo-nido*-$\{Rh(PR_3)_2\}^+$ fragment plays an important part in the catalytic cycle. More recently, Teixidor and co-workers have extended this idea by using tethered *exo-nido*-monophosphinorhodacarboranes and -monothiorhodacarboranes,[30−33] while other workers have also contributed to the area, especially in enantioselective catalysis using rhodacarboranes.[34,35] In general, all these catalysts show good activities for the hydrogenation of terminal olefins such as 1-hexene[23,25,30] at room temperature and pressure, while to effect the efficient hydrogenation of internal alkenes, such as cyclohexene, elevated pressures are required (ca. 20 atm).[33]

Given the stated methodological gap in the ability of rhodium phosphines to hydrogenate internal alkenes efficiently, an obvious synthetic target is a rhodium complex that might compete with iridium catalysts in the hydrogenation of relatively hindered internal alkenes under the attractive conditions of room temperature and pressure. The question we were interested in asking was whether this could be realized by changing the counterion from $[BF_4]^-$ or $[PF_6]^-$ to one derived from [*closo*-$CB_{11}H_{12}]^-$, on the basis that the technological advances in performance made with rhodium-based systems (i.e. chiral ligands, precatalyst design, mechanistic elucidation) could be incorporated directly into new, potentially more efficient catalysts. In this contribution we report the synthesis and characterization of new rhodium catalyst precursors based around the anions [*closo*-$CB_{11}H_{12}]^-$ (**I**) and [*closo*-$CB_{11}H_6Br_6]^-$ (**II**) (Chart 1), and their subsequent evaluation as olefin hydrogenation catalysts. We demonstrate that this methodology affords complexes that are broadly competitive with Crabtree's catalyst in the room-temperature and -pressure hydrogenation of the internal alkenes cyclohexene, 1-methylcyclohexene, and 2,3-dimethyl-2-butene.

Results

Our initial synthetic goal was to prepare representative examples of rhodium phosphine complexes partnered with anions **I** and **II**, affording complexes that are active precatalysts for olefin hydrogenation. In such complexes, the weakly coordinating carborane anion could, in principle, easily move to one side to allow olefin and dihydrogen to coordinate to the rhodium, while remaining available in order to stabilize any unsaturated metal center in a catalytic cycle by B−H−M or B−Br−M interactions. Given the established ability for carborane monoanions, especially the perhalogeno derivatives, to stabilize reactive cationic species[18,36−39] and reveal faster rates in Lewis acid catalyzed reactions,[22,40] we have synthesized precatalysts based on the Schrock−Osborn cationic system, of the general formula $\{[(PPh_3)_2Rh][Y]\}_n$ (L = PPh_3; Y = [*closo*-$CB_{11}H_{12}$], $n = 1$; Y = [*closo*-$CB_{11}H_6Br_6$], $n = 2$). These have been synthesized by two routes: silver salt metathesis and hydrogenation of a precursor norbornadiene complex.

Silver Salt Metathesis. Reaction of 1 equiv of $[(PPh_3)_2RhCl]_2$ with Ag[*closo*-$CB_{11}H_{12}$] affords a red solution from which the new complex $[(PPh_3)_2Rh$(*closo*-$CB_{11}H_{12})]$ (**1**) can be isolated in good yield as crystalline material. The solid-state structure of complex **1** is shown in Figure 1, with salient bond lengths and angles given in Table 2.

An X-ray diffraction study demonstrates that the $\{Rh(PPh_3)_2\}^+$ fragment is bound to the periphery of the cage by two B−H−Rh three-center−two-electron bonds. Exopolyhedrally coordinated $\{Rh\text{-}L_2\}^+$ (L = two-electron donor) fragments with carborane anions have been reported previously. For example, we have recently

(17) Strauss, S. H. *Chem. Rev.* **1993**, *93*, 927.
(18) Reed, C. A. *Acc. Chem. Res.* **1998**, *31*, 133.
(19) Patmore, N. J.; Steed, J. W.; Weller, A. S. *Chem. Commun.* **2000**, 1055.
(20) Patmore, N. J.; Mahon, M. F.; Steed, J. W.; Weller, A. S. *J. Chem. Soc., Dalton Trans.* **2001**, 277.
(21) Weller, A. S.; Mahon, M. F.; Steed, J. W. *J. Organomet. Chem.* **2000**, *614−615*, 113.
(22) Hague, C.; Patmore, N. J.; Frost, C. G.; Mahon, M. F.; Weller, A. S. *Chem. Commun.* **2001**, 2286.
(23) Delaney, M. S.; Knobler, C. B.; Hawthorne, M. F. *Chem. Commun.* **1980**, 849.
(24) Baker, R. T.; Delaney, M. S.; King, R. E., III; Knobler, C. B.; Long, J. A.; Marder, T. B.; Paxson, T. E.; Teller, R. G.; Hawthorne, M. F. *J. Am. Chem. Soc.* **1984**, *106*, 2965.
(25) Behnken, P. E.; Belmont, J. A.; Busby, D. C.; Delaney, M. S.; King, R. E., III; Kreimendahl, C. W.; Marder, T. B.; Wilczynski, J. J.; Hawthorne, M. F. *J. Am. Chem. Soc.* **1984**, *106*, 3011.
(26) Knobler, C. B.; Marder, T. B.; Mizusawa, E. A.; Teller, R. G.; Long, J. A.; Behnken, P. E.; Hawthorne, M. F. *J. Am. Chem. Soc.* **1984**, *106*, 2990.
(27) Long, J. A.; Marder, T. B.; Behnken, P. E.; Hawthorne, M. F. *J. Am. Chem. Soc.* **1984**, *106*, 2979.
(28) Long, J. A.; Marder, T. B.; Hawthorne, M. F. *J. Am. Chem. Soc.* **1984**, *106*, 3004.
(29) Belmont, J. A.; Soto, J.; King, R. E., III; Donaldson, A. J.; Hewes, J. D.; Hawthorne, M. F. *J. Am. Chem. Soc.* **1989**, *111*, 7475.
(30) Teixidor, F.; Flores, M. A.; Viñas, C.; Kivekäs, R.; Sillanpää, R. *Angew. Chem., Int. Ed. Engl.* **1996**, *35*, 2251.
(31) Teixidor, F.; Flores, M. A.; Viñas, C.; Kivekäs, R.; Sillanpää, R. *Organometallics* **1998**, *17*, 4675.
(32) Viñas, C.; Flores, M. A.; Núñez, R.; Teixidor, F.; Kivekäs, R.; Sillanpää, R. *Organometallics* **1998**, *17*, 2278.
(33) Teixidor, F.; Flores, M. A.; Viñas, C.; Sillanpää, R.; Kivekäs, R. *J. Am. Chem. Soc.* **2000**, *122*, 1963.
(34) Pirotte, B.; Felekidis, A.; Fontaine, M.; Demonceau, A.; Noels, A. F.; Delarge, J.; Chizhevesky, I. T.; Zinevich, T. V.; Pisareve, I. V.; Bregadze, V. I. *Tetrahedron Lett.* **1993**, *34*, 1471.
(35) Brunner, H.; Apfelbacher, A.; Zabel, M. *Eur. J. Inorg. Chem.* **2001**, 917.
(36) Xie, Z. W.; Manning, J.; Reed, R. W.; Mathur, R.; Boyd, P. D. W.; Benesi, A.; Reed, C. A. *J. Am. Chem. Soc.* **1996**, *118*, 2922.
(37) Reed, C. A.; Fackler, N. L. P.; Kim, K. C.; Stasko, D.; Evans, D. R.; Boyd, P. D. W.; Rickard, C. E. F. *J. Am. Chem. Soc.* **1999**, *121*, 6314.
(38) Reed, C. A.; Kim, K. C.; Bolskar, R. D.; Mueller, L. J. *Science* **2000**, *289*, 101.
(39) Lupinetti, A. J.; Havighurst, M. D.; Miller, S. M.; Anderson, O. P.; Strauss, S. H. *J. Am. Chem. Soc.* **1999**, *121*, 11920.
(40) Dubay, W. J.; Grieco, P. A.; Todd, L. J. *J. Org. Chem.* **1994**, *59*, 6898.

Chart 1

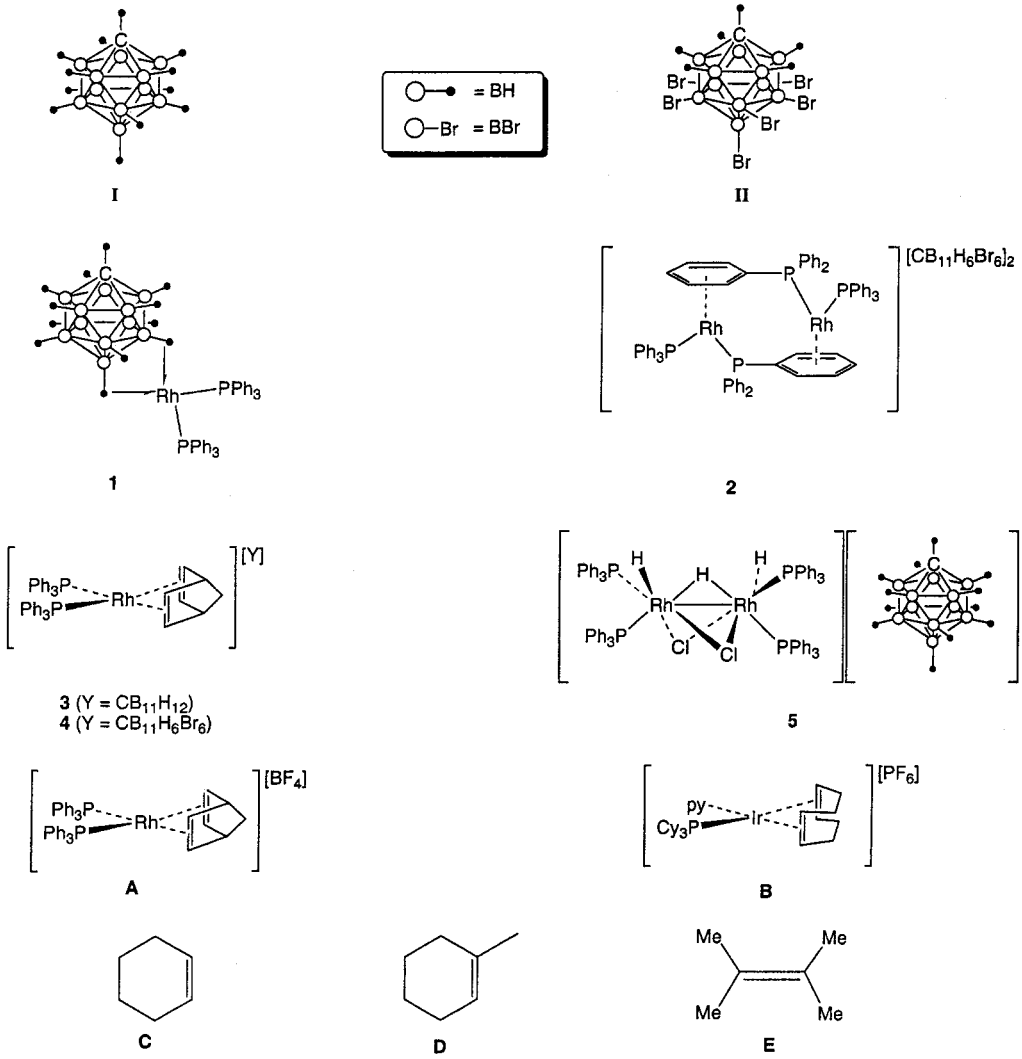

reported the synthesis and solid-state structure of [(cod)Rh(*closo*-$CB_{11}H_{12}$)],[21] while structures incorporating *nido*-{C_2B_9} cages, such as [*exo*-*nido*-{$Rh(PPh_3)_2$}-7-Me-8-Ph-7,8-$C_2B_9H_{10}$],[26] [Rh(7-SR-8-R′-7,8-$C_2B_9H_{10}$)(cod)],[33] and [10-*endo*-{$Au(PPh_3)$}-5,10-(μ-H)$_2$-*exo*-{$Rh(PPh_3)_2$}-7,8-Me_2-*nido*-$C_2B_9H_7$],[41] are well-established. The spectroscopic characterization of the related complex [Re$(CO)_3$-*exo*-{$Rh(PPh_3)_2$}-7,8-Me_2-*nido*-7,8-$C_2B_9H_9$] has also been reported.[42] The $\{Rh(PPh_3)_2\}^+$ fragment in **1** is coordinated with the cage via two three-center−two-electron bonds through {BH(12)} and {BH(7)}, giving the molecule approximate C_s symmetry, similar to that observed for [(cod)Rh(*closo*-$CB_{11}H_{12}$)], and is as expected on the basis of charge distribution in the cage.[43] Although the location of the {CH} vertex in carboranes can sometimes be problematic, C(1) was located unambiguously by inspection of its thermal parameters and bond lengths to neighboring atoms. The two Rh−B distances are similar, Rh(1)−B(7) = 2.359(3) Å and Rh(1)−B(12) = 2.407(3) Å. These bond lengths are comparable to those observed in [(cod)Rh(*closo*-$CB_{11}H_{12}$)]: viz., 2.391(3) and 2.385(3) Å. The rhodium center in **1** is pseudo square planar coordinated, as reflected in the P(1)−P(2)−B(12)−B(7) dihedral angle of 7.35°. All other bond lengths and angles in **1** are within the ranges expected and are unremarkable.

In solution, the solid-state structure of **1** is not retained. The $\{Rh(PPh_3)_2\}^+$ fragment is fluxional over the lower surface of the cage on the NMR time scale, which is evidenced by local C_{5v} symmetry for the cage being observed in both the $^{11}B\{^1H\}$ and $^1H\{^{11}B\}$ NMR spectra. Thus, three environments are seen in the $^{11}B\{^1H\}$ NMR spectrum, at δ −9.9, −13.5, and −14.1, in the ratio 1:5:5. This pattern is also mirrored in the B−H region of the $^1H\{^{11}B\}$ NMR spectrum. Coordination of a metal fragment to [*closo*-$CB_{11}H_{12}]^-$ generally results in a diagnostic upfield shift of those {BH} vertexes involved in bonding,[19,21] and the room-temperature $^{11}B\{^1H\}$ and $^1H\{^{11}B\}$ NMR spectra of complex **1** reflect this by a shift of the signals assigned to the {BH(12)} vertex and the lower pentagonal belt {BH} vertexes, B(7) to B(11), compared with Ag[$CB_{11}H_{12}$].[20] In particular, the unique antipodal {BH} unit is observed at δ −1.97 in the $^1H\{^{11}B\}$ NMR spectrum, which becomes a well-resolved quartet with a reduced value for the BH coupling constant (J(BH) = 119 Hz) in the ^1H NMR spectrum. This is consistent with coordination of a metal fragment and reduction of the B−H bond

(41) Jeffery, J. C.; Jelliss, P. A.; Stone, F. G. A. *J. Chem. Soc., Dalton Trans.* **1993**, 1073.
(42) Ellis, D. D.; Jellis, P. A.; Stone, F. G. A. *Organometallics* **1999**, *18*, 4982.
(43) Hoffmann, R.; Lipscomb, W. N. *J. Chem. Phys.* **1962**, *36*, 3489.

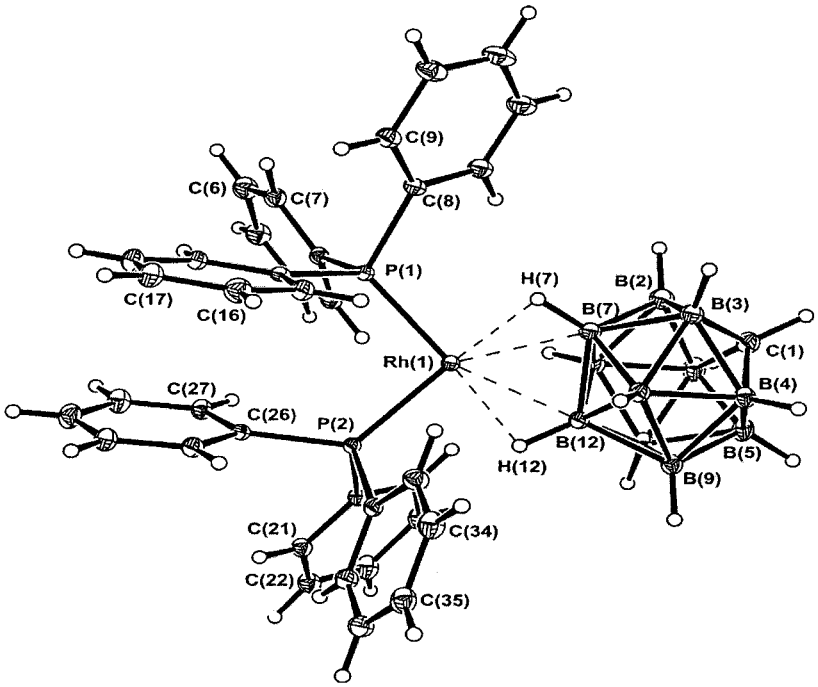

Figure 1. ORTEX drawing of complex **1**. Thermal ellipsoids are drawn at the 30% probability level.

Table 1. Crystal Data and Structure Refinement for Complexes 1, 2, and 5

	1	**2**	**5**
empirical formula	$C_{37}H_{42}B_{11}P_2Rh$	$C_{74}H_{72}B_{22}Br_{12}P_4Rh_2 \cdot 2.78CH_2Cl_2$	$C_{74}H_{77}B_{11}Cl_4P_4Rh_2$
fw	770.47	2723.85	1556.77
T/K	293(2)	150(2)	150(2)
cryst syst	monoclinic	monoclinic	monoclinic
space group	$P2_1/c$	$C2/c$	$P2_1/n$
a/Å	9.22630(10)	26.9570(6)	20.5720(7)
b/Å	14.5292(2)	15.0290(4)	16.3620(5)
c/Å	28.4345(3)	27.8970(7)	21.5570(8)
α/deg	90	90	90
β/deg	93.3510(6)	113.284(2)	90.699(2)
γ/deg	90	90	90
U/Å^3	3805.15(8)	10381.6(4)	7255.5(4)
Z	4	4	4
μ/mm^{-1}	0.561	5.181	0.733
no. of rflns collected	57 907	72 519	53 162
no. of indep rflns	8703 ($R_{int} = 0.0468$)	9133 ($R_{int} = 0.1239$)	12 705 ($R_{int} = 0.2739$)
final R1, wR2 indices			
$I > 2\sigma(I)$	0.0309, 0.0850	0.0699, 0.1261	0.0827, 0.1358
all data	0.0447, 0.1048	0.1247, 0.1471	0.1886, 0.1742

strength.[44] The lower pentagonal belt hydrogen atoms are observed as a broader quartet shifted upfield to δ 0.1; while the upper belt hydrogens, which are not involved with metal binding, are essentially unshifted. The fluxional process also renders the phosphine ligands equivalent on the NMR time scale, with one environment being observed at δ 49.0 (J(RhP) = 194 Hz). These observations are consistent with the mechanism previously proposed for the dynamic process occurring with other {L_2M} fragments coordinated to [*closo*-$CB_{11}H_{12}]^-$,[21,45] [*nido*-$C_2B_9H_{11}]^-$,[26] or its derivatives.[42]

Reaction of $[(PPh_3)_2RhCl]_2$ with 1 equiv of Ag[*closo*-$CB_{11}H_6Br_6$] affords a red solution which, after filtration, contains only one compound, spectroscopically identified as $[(PPh_3)_2Rh(\eta^6\text{-}C_6H_5Me)][CB_{11}H_6Br_6]$ by a doublet at δ 45.1 (J(RhP) = 206 Hz) in the $^{31}P\{^1H\}$ NMR spectrum and characteristic signals due to coordinated arene in the ^1H NMR spectrum. These chemical shifts and coupling constants are similar to those reported for $[(dppe)Rh(\eta^6\text{-}C_6H_6)][BF_4]$,[46] and we presume that the coordinated toluene arises from residual solvent left over from the preparation of $[(PPh_3)_2RhCl]_2$. In our hands, repeated washing of the starting material did not completely remove toluene and the arene-coordinated cation persisted. Employing $[(PPh_3)_2RhCl]_2$ prepared using methyl ethyl ketone as solvent[47] gave a mixture of products, although the toluene-coordinated complex was absent. We have not actively pursued the complete identification of all the components of this mixture, but we could assign the major species as being the arene-bridged dimer complex $[(Ph_3P)\{PPh_2(\eta^6\text{-}C_6H_5)\}Rh]_2$-

(44) Crowther, D. J.; Borkowsky, S. L.; Swenson, D.; Meyer, T. Y.; Jordan, R. F. *Organometallics* **1993**, *12*, 2897.
(45) Mhinzi, G. S.; Litster, S. A.; Redhouse, A. D.; Spencer, J. L. *J. Chem. Soc., Dalton Trans.* **1991**, 2769.
(46) Singewald, E. T.; Slone, C. S.; Stern, C. L.; Mirkin, C. A.; Yap, G. P. A.; Liable-Sands, L. M.; Rheingold, A. L. *J. Am. Chem. Soc.* **1997**, *119*, 3048.
(47) Osborn, J. A.; Jardine, F. H.; Young, J. F.; Wilkinson, G. *J. Chem. Soc. A* **1966**, 1711.

Scheme 1

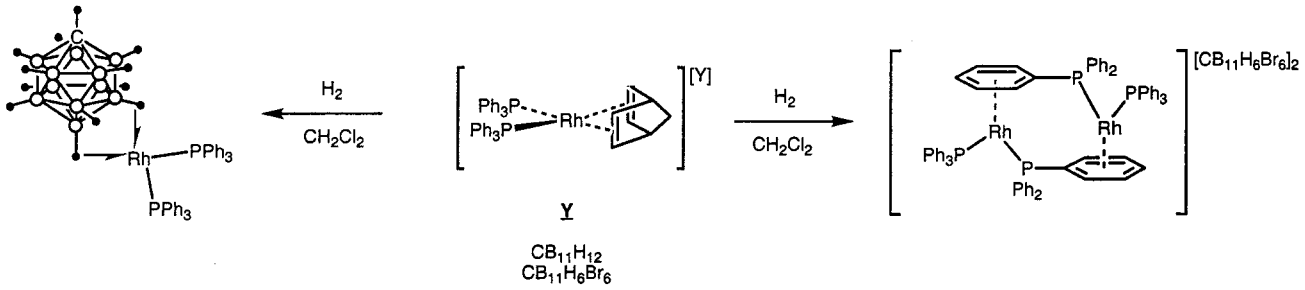

Table 2. Selected Interatomic Distances (Å) and Angles (deg) for Compounds 1, 2, and 5

	Compound **1**		
Rh(1)−P(1)	2.2192(6)	Rh(1)−P(2)	2.2391(6)
Rh(1)−B(7)	2.359(3)	Rh(1)−B(12)	2.407(3)
P(1)−Rh(1)−P(2)	95.73(2)	P(1)−Rh(1)−B(7)	113.88(7)
P(2)−Rh(1)−B(7)	150.39(7)	P(1)−Rh(1)−B(12)	155.46(6)
P(2)−Rh(1)−B(12)	107.98(6)	B(7)−Rh(1)−B(12)	42.57(9)
	Compound **2**		
Rh(1)−P(1)	2.248(2)	Rh(1)−P(2)	2.262(3)
Rh(1)−C(2)	2.399(8)	Rh(1)−C(3)	2.365(8)
Rh(1)−C(4)	2.269(8)	Rh(1)−C(5)	2.333(9)
Rh(1)−C(6)	2.316(9)	Rh(1)−C(7)	2.254(8)
Rh(1)−P(1)	2.247(2)	Rh(1)−P(2)	2.262(2)
Rh(1)−Br(7)	5.848(1)		
Rh(1)−P(1)−C(2)	108.9(3)	P(1)−Rh(1)−P(2)	95.96(8)
	Compound **5**		
Rh(1)−Rh(2)	2.776(1)	Rh(1)−H(1)	1.59(7)
Rh(2)−H(2)	1.60(9)	Rh(1)−H(3)	1.82(6)
Rh(2)−H(3)	1.82(6)	Rh(1)−P(1)	2.257(3)
Rh(1)−P(2)	2.313(3)	Rh(2)−P(3)	2.257(3)
Rh(2)−P(4)	2.301(3)	Rh(1)−Cl(1)	2.416(3)
Rh(1)−Cl(2)	2.553(2)	Rh(2)−Cl(1)	2.538(3)
Rh(2)−Cl(2)	2.394(2)		
Rh(1)−Cl(1)−Rh(2)	68.11(7)	Rh(1)−Cl(2)−Rh(2)	68.19(7)
Rh(1)−H(3)−Rh(2)	99(3)	P(1)−Rh(1)−P(2)	99.01(9)
P(3)−Rh(1)−P(4)	102.3(1)		
H(1)−Rh(1)−Cl(2)	163(3)	H(2)−Rh(2)−Cl(1)	168(4)

[*closo*-$CB_{11}H_6Br_6$]$_2$, which can be prepared quantitatively using an alternative method (vide infra). Given that the silver salt metathesis route using Ag[*closo*-$CB_{11}H_6Br_6$] did not give a clean reaction, an alternative method was used to generate precatalyst partnered with this weakly coordinating anion.

Norbornadiene Precursor Complexes. An attractive aspect of cationic Schrock−Osborn rhodium catalysts is that air-stable precatalysts such as [(L)$_2$Rh(nbd)][PF_6] (L = phosphine) can be readily prepared. In coordinating solvents the active hydrogenation catalyst [(L)$_2$RhH_2(solvent)$_2$][PF_6] is straightforwardly produced by treating a solution of these olefin complexes with 1 atm of hydrogen.[2] In noncoordinating solvents, such as dichloromethane, treatment of [(L$_2$)Rh(nbd)][BF_4] (L$_2$ = chelating diphosphine) affords dimeric species with bridging arene groups.[48,49] With relatively more coordinating anions than [BF_4]$^-$ or [PF_6]$^-$, such as perchlorate or sulfonates, monomeric species are suggested to occur.[14,49] When the counterion also contains phenyl groups, arene-bound zwitterions such as (η^6-PhBPh_3)Rh(dppb) (dppb = diphenylphosphinobutane) can be formed.[50] The kinetic aspects of the hydrogenation of alkenes and alkynes by [(PPh_3)$_2$Rh(nbd)][BF_4] in noncoordinating solvents such as CH_2Cl_2 has also been discussed.[51,52]

Treatment of a dichloromethane solution of the new complex [(PPh_3)$_2$Rh(nbd)][*closo*-$CB_{11}H_{12}$] (**3**) with H_2 (1 atm) for 10 min resulted in a color change from orange to red. After removal of volatiles in vacuo, NMR spectroscopy (^{1}H, ^{31}P{^{1}H}, and ^{11}B{^{1}H}) showed that compound **1** is formed essentially quantitatively (Scheme 1). This puts [*closo*-$CB_{11}H_{12}$]$^-$ in the same league as anions such as sulfonates and perchlorate with regard to coordinating ability, as all of these anions can form complexes with {L_2Rh}$^+$ fragments. In contrast, exposure of [(PPh_3)$_2$Rh(nbd)][*closo*-$CB_{11}H_6Br_6$] (**4**) to H_2 in dichloromethane affords a claret-colored solution from which the dimeric species [(PPh_3)(PPh_2-η^6-C_6H_5)Rh]$_2$-[*closo*-$CB_{11}H_6Br_6$]$_2$ (**2**) can be isolated as an air-sensitive crystalline solid. Compound **2** was characterized by solution NMR spectroscopy and a single-crystal X-ray diffraction study and shown to have a structure in which an arene ring from one of the phosphines on each rhodium bridges to the second metal center in the cation. The isolation of the dimeric species with [*closo*-$CB_{11}H_6Br_6$]$^-$ is in agreement with the relative weakly coordinating abilities of this anion compared with [*closo*-$CB_{11}H_{12}$]$^-$ [18] and other anions.[20,53] Conversion of **4** to **2** is essentially quantitative (by NMR).

Comparison of the ^{1}H and ^{13}P{^{1}H} NMR spectra of **2** with those of other reported complexes that contain η^6-arene-bridged structures shows close similarities.[49,54] Specifically, the observation of diagnostic peaks between δ 5.32 and 7.43 in the ^{1}H NMR spectrum is strongly indicative of the proposed arene-bridged structure. In the ^{31}P{^{1}H} NMR spectrum two environments are observed at δ 44.6 and 47.5, which show coupling to ^{31}P and ^{103}Rh in a second-order AA′BB′XX′ system, again consistent with previously reported arene-bridged complexes containing chelating phosphine ligands.[54] The ^{31}P{^{1}H} NMR spectrum of complex **2** may be simulated satisfactorily using the program gNMR[55] (see Supporting Information). Inspection of the ^{1}H{^{11}B} NMR spectrum confirmed the ratio of phosphines to cage as 2:1. Although such bridged arene structures have been

(48) Halpern, J.; Riley, D. P.; Chan, A. S. C.; Pluth, J. J. *J. Am. Chem. Soc.* **1977**, *99*, 8055.
(49) Fairlie, D. P.; Bosnich, B. *Organometallics* **1988**, *7*, 936.
(50) Zhou, Z.; Facey, G.; James, B. R.; Alper, H. *Organometallics* **1996**, *15*, 2496.
(51) Esteruelas, M. A.; González, I.; Herrero, J.; Oro, L. A. *J. Organomet. Chem.* **1998**, *551*, 49.
(52) Esteruelas, M. A.; Herrero, J.; Martín, M.; Oro, L. A.; Real, V. M. *J. Organomet. Chem.* **2000**, *599*, 178.
(53) Evans, D. R.; Reed, C. A. *J. Am. Chem. Soc.* **2000**, *122*, 4660.
(54) Allen, D. G.; Wild, S. B.; Wood, D. L. *Organometallics* **1986**, *5*, 1009.
(55) Budzelaar, P. gNMR; Cherwell Scientific Publishing, Oxford, U.K., 1997.

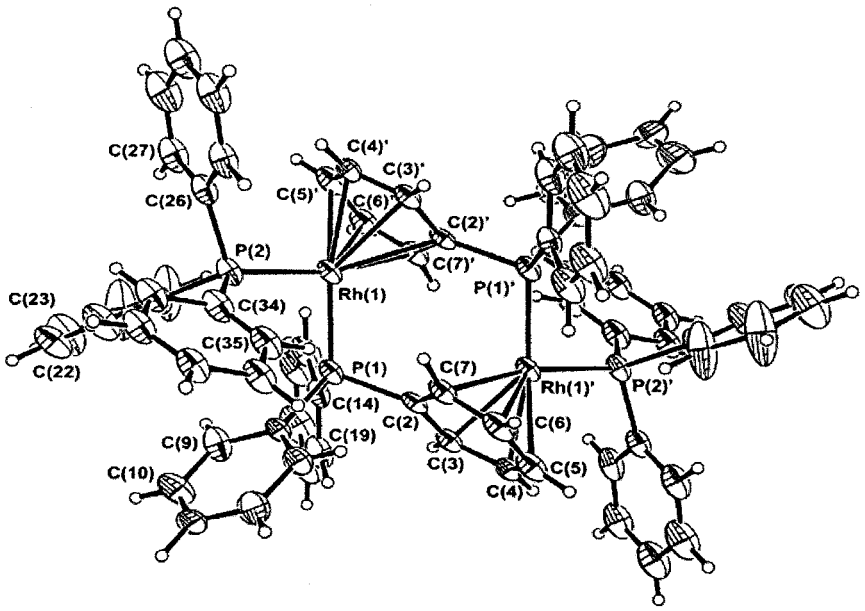

Figure 2. ORTEX drawing of the dicationic portion of complex **2**. Thermal ellipsoids are drawn at the 30% probability level. The disorder present in phenyl ring C(32)−C(37) and its symmetry equivalent is not shown, with only the major component (65% occupancy) drawn.

Table 3. Catalytic Hydrogenation of Selected Alkenes Using Complexes 3, 4, I, and II[a]

entry	catalyst	substrate	time, h	yield,[b] %	TOF, h^{-1}
1	$[(PPh_3)_2Rh(nbd)][CB_{11}H_{12}]$ **(3)**	cyclohexene	2	43	22
2	$[(PPh_3)_2Rh(nbd)][CB_{11}H_6Br_6]$ **(4)**	cyclohexene	<0.5	100	>200
3	$[(PPh_3)_2Rh(nbd)][BF_4]$ **(A)**	cyclohexene	2	29	15
4	$[(PPh_3)_2Rh(nbd)][CB_{11}H_{12}]$ **(3)**	1-methyl-1-cyclohexene	6	4	0.7
5	$[(PPh_3)_2Rh(nbd)][CB_{11}H_6Br_6]$ **(4)**	1-methyl-1-cyclohexene	5	95	19
6	$[(py)(PCy_3)Ir(cod)][PF_6]$ **(B)**	1-methyl-1-cyclohexene	5	100	20
7	$[(PPh_3)_2Rh(nbd)][CB_{11}H_6Br_6]$ **(4)**	2,3-dimethylbut-2-ene	24	68	3
8	$[(py)(PCy_3)Ir(cod)][PF_6]$ **(B)**	2,3-dimethylbut-2-ene	16	95	6

[a] Conditions: catalyst, 1 mol %; CH_2Cl_2 5 cm^3; H_2, 10 psi; temperature, 20 °C. [b] Yields quoted are the average of two runs and were determined by GC.

established in the literature for some time, to our knowledge compound **2** is the first example isolated using a monodentate phosphine. A single-crystal X-ray diffraction study was therefore undertaken to confirm the structure, for which an ORTEX[56] representation is given in Figure 2. Despite repeated attempts, only very small, poorly shaped crystals of **2** could be grown, and consequently the final refinement is not as good as we would traditionally expect from data collected on our diffractometers. Nevertheless, the gross structural features of the molecule can be seen, even if discussion of individual bond lengths and angles is not appropriate.

The solid-state structure of **2** supports the solution NMR data, in that each rhodium center is bound to two PPh_3 ligands, one of which bridges to another rhodium center via an η^6 interaction, resulting in a formal 18-electron count at each metal center. The molecule crystallizes with a crystallographically imposed inversion center. The two carborane anions do not interact with the metal centers, the shortest Rh···Br distance being 5.85 Å. It is of note that the room-temperature ^1H NMR spectrum shows a particularly high-field-shifted resonance of one of the bridging arene protons, at δ 5.32, and we assign this to the hydrogen atom H(4) and its symmetry equivalent in the solid-state structure which lies approximately over the center of the phenyl ring C(26)−C(31).

(56) McArdle, P. *J. Appl. Crystallogr.* **1995**, *28*, 65.

Catalytic Hydrogenations. The precatalysts **3** and **4** have been tested for their efficiency in the hydrogenation of the internal alkenes: cyclohexane (**C**), 1-methylcyclohex-1-ene (**D**), and 2,3-dimethylbut-2-ene (**E**), which are progressively more sterically hindered and have historically not been suitable substrates for cationic $[(R_3P)_2Rh(nbd)]^+$-based catalysts under ambient laboratory conditions. Hydrogenation reactions were performed at room temperature under 10 psi of hydrogen pressure in Schlenk tubes fitted with septa, using 1 mol % of catalyst in ca. 5 cm^3 of CH_2Cl_2. The catalytic activity of $[(PPh_3)_2Rh(nbd)][BF_4]$ (**A**) and Crabtree's catalyst $[(py)(PCy_3)Ir(cod)][PF_6]$ (**B**) under the conditions used by us for the evaluation of the new catalyst here have been included for comparison. Table 3 summarizes selected results from this investigation.

The data presented in Table 3 show that changing the counterion from [*closo*-$CB_{11}H_{12}]^-$ to [*closo*-$CB_{11}H_6Br_6]^-$ results in a dramatic effect on both the overall yield of hydrogenated product and the turnover frequency (TOF). While precatalyst **3** (and thus complex **1** on initial hydrogenation) gives modest yields of saturated product for cyclohexene after 2 h (entry 1), precatalyst **4** (giving complex **2** on initial hydrogenation) affords complete hydrogenation of cyclohexene to cyclohexane in under 30 min (entry 2), with an concomitant order of magnitude difference in TOF compared with **3** on changing the counterion from [*closo*-$CB_{11}H_{12}]^-$ to

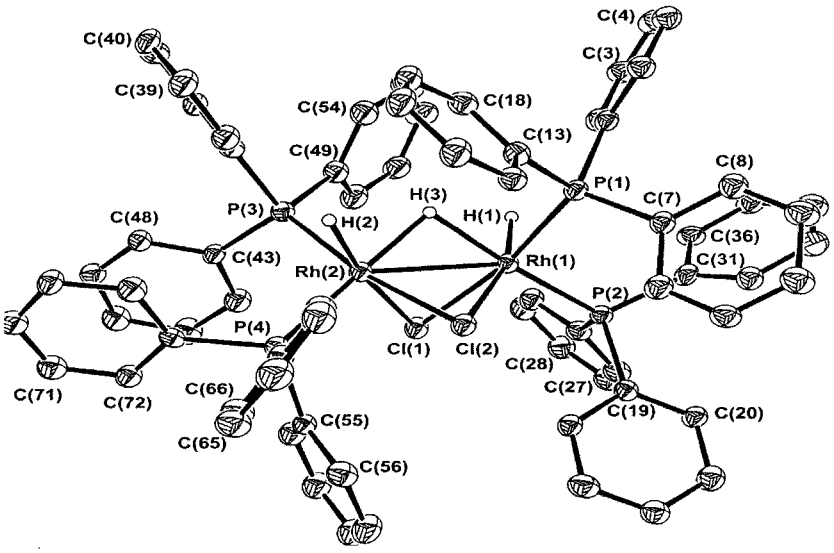

Figure 3. ORTEX drawing of the cationic portion of complex **5**. Thermal ellipsoids are drawn at the 30% probability level. Hydrogen atoms, apart from those associated with the rhodium metal centers, are omitted for clarity.

[*closo*-$CB_{11}H_6Br_6$]$^-$. When $[BF_4]^-$ is used as the counterion (entry 3), the yield of hydrogenated product is comparable to that of **3** but significantly smaller than that of **4**. Moving to the more sterically hindered olefin 1-methyl-1-cyclohexene, the effect of anion is even more pronounced (entries 4 and 5). After 5 h almost complete conversion (95%) is observed with **4**, while complex **3** barely effects hydrogenation. For comparison we have tested Crabtree's catalyst under these conditions and find that complete hydrogenation of **D** is effected after 5 h (entry 6). Even with the sterically very hindered alkene 2,3-dimethylbut-2-ene, complex **4** effects 68% conversion to the alkane (entry 7). Although this is not as good as we find for Crabtree's catalyst (entry 8), as far as we are aware this is excellent for a rhodium catalyst under the benign conditions of room temperature and pressure. Comparable activities have recently been reported for neutral β-diimine rhodium complexes, hydrogenation in this case being performed in neat olefin.[57]

Deactivation Product. The fact that the reduction of the hindered alkene 2,3-dimethyl-but-2-ene did not go to completion suggested that a catalytically inactive complex is formed during hydrogenation, similar to the dimeric and trimeric hydride-bridged iridium cations, such as $[Ir_2H_5(PPh_3)_4]^+$ and $[Ir_3H_7(PCy_3)_3(py)_3]^+$, that are the deactivation products with Crabtree's catalyst and related complexes[7] or the catalytically inactive dimeric rhodium complexes formed on hydrogenation of Schrock−Osborn type systems.[16] A ^{1}H NMR spectrum of the residue from the hydrogenation of 2,3-dimethylbut-2-ene with preacatalyst **4** shows that there is one major organometallic product (ca. 95%). Initially we partially characterized this as the cationic hydride- and halide-bridged dimer $[(PPh_3)_2HRh(\mu\text{-}Cl)_2(\mu\text{-}H)RhH(PPh_3)_2]$[*closo*-$CB_{11}H_6Br_6$] ((**5**)[$CB_{11}H_6Br_6$]) by multinuclear NMR spectroscopy. The structure was only ultimately resolved by a single-crystal X-ray analysis of the [*closo*-$CB_{11}H_{12}$]$^-$ salt, which was formed by treatment of a CH_2Cl_2 solution of **3** with H_2 over 4 days to afford (**5**)[*closo*-$CB_{11}H_{12}$] as the major product. Although we have isolated single crystals of the [*closo*-$CB_{11}H_{12}$]$^-$ salt, NMR data are identical for both anions, disregarding the resonances associated with the cage hydrogen atoms, demonstrating that they adopt the same structural motif. An ORTEX representation of (**5**)[$CB_{11}H_{12}$] is shown in Figure 3.

The complex (**5**)[$CB_{11}H_{12}$] is a cationic 34-CVE dimer, with a Rh−Rh distance that suggests a significant metal−metal interaction (2.776(1) Å). Each rhodium is spanned by two chloride atoms and one hydride ligand, while one terminal hydride is found on each metal center along with two PPh_3 ligands. The hydrides were located in the difference map and their positions confirmed by NMR data. The terminal hydride ligands are orientated in an anti configuration with respect to the Rh−Rh vector, giving the molecule approximate, noncrystallographic C_2 symmetry. One carborane anion is located in the unit cell, giving the metal complex an overall positive charge. This makes each metal center formally Rh^{3+}, consistent with the observed diamagnetism. The Rh−Rh distance is in the range associated with dinuclear rhodium complexes with a metal−metal bond.[58−60] The two chloride ligands do not span the Rh−Rh vector symmetrically, one Rh−Cl distance in each Rh−Cl−Rh unit being significantly longer than the other: viz., Rh(2)−Cl(1) = 2.538(3) Å and Rh(1)−Cl(1) = 2.416(3) Å. This difference can be traced back to the approximate trans orientation of the terminal hydrides with respect to the chloride ligands (H(2)−Rh(2)-Cl(1) = 168(4)° and H(1)−Rh(1)−Cl(2) = 163(3)°), meaning that each bridging chloride is approximately trans to both a phosphine and a hydride, with a resulting differential in the observed Rh−Cl bond lengths. Similarly, the phosphine trans to the bridging hydride on each rhodium has a slightly longer Rh−P bond length: Rh(1)−P(1) = 2.257(3) Å and Rh(1)−P(2) = 2.313(3) Å. The complex (**5**)[$CB_{11}H_{12}$] is closely related to the

(57) Budzelaar, P.; Moonen, N. N. P.; De Gelder, R.; Smits, J. M. M.; Gal, A. W. *Eur. J. Inorg. Chem.* **2000**, 753.

(58) Herrmann, W. A. *Adv. Organomet. Chem.* **1982**, *20*, 159.
(59) Isoke, K.; Vázquez De Miguel, A.; Bailey, P. M.; Okeya, S.; Maitlis, P. M. *J. Chem. Soc., Dalton Trans.* **1983**, 1441.
(60) Koizumi, T.; Osakada, K.; Yamamoto, T. *Organometallics* **1998**, *17*, 5721.

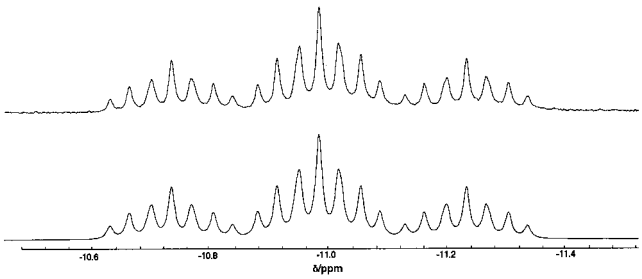

Figure 4. Experimental (top) and simulated (bottom) ^{1}H NMR spectra for the bridging hydride region in the cation $[(PPh_3)_2RhH(\mu\text{-}H)(\mu\text{-}Cl)_2HRh(PPh_3)_2]^+$.

structurally characterized $[Ir_2H_5(PPh_3)_4]^+$,[7] apart from the replacement of two bridging hydrides in the iridium complex by chlorides, which must originate from the dichloromethane solvent used in the hydrogenation reactions. In addition, the cation $[\mathbf{5}]^+$ is the rhodium congener of $[Ir_2(H(PPh_3)_2)_2(\mu\text{-}H)(\mu\text{-}Cl)_2]^+$ formed from addition of HCl to $[Ir(H(PPh_3)_2)(\mu\text{-}H)_3]^+$.[61,62] Attempts to avoid dimer formation by hydrogenation in THF rather than dichloromethane led only to low activities (ca. 10% for cyclohexene, [*closo*-$CB_{11}H_6Br_6$] counterion) in this coordinating solvent. In addition to dimeric rhodium hydride compounds previously observed as deactivation products in Schrock−Osborn type systems, dimeric complexes formed on hydrogenation of rhodacarboranes have been reported previously,[23] while, in contrast, certain exo-substituted rhodacarboranes have been shown to be recoverable after catalytic hydrogenation in toluene or THF.[32]

With the identity of the cation $[\mathbf{5}]^+$ in hand, the ^{1}H and ^{31}P NMR spectra can be confidently interpreted as being fully consistent with the solid-state structure. The $^{31}P\{^1H\}$ NMR spectrum displays two strongly second-order coupled resonances at δ 36.0 and δ 51.5, corresponding to the two phosphine environments in $[\mathbf{5}]^+$. The spectrum has been successfully simulated as an AA′BB′XX′ spin system (see the Supporting Information). In the hydride region of the ^{1}H NMR spectrum two resonances are observed in the ratio 1:2 at δ −11.0 and −16.5, assigned to the bridging and terminal hydrides, respectively. The latter resonance is observed as an apparent quartet (doublet of doublet of doublets), showing coupling to one ^{103}Rh center and two ^{31}P nuclei, which simplifies to a doublet in the $^1H\{^{31}P\}$ NMR spectrum. The fact that no $^1H-^1H$ coupling is observed (or it is very close to 0 Hz) was confirmed by a selected homonuclear decoupling experiment that showed no change in peak pattern or intensity for either of the hydride peaks on irradiation of the other. The bridging hydride at δ −11.0 is observed as a complicated multiplet that resembles a triplet of septets, which simplifies to a binomial triplet in the $^1H\{^{31}P\}$ NMR spectrum, thus confirming the Rh−H−Rh motif. The coupling pattern has been successfully simulated as a AA′BB′MXX′ spin system (Figure 4) (full details of the resolved coupling constants are given in the Supporting Information). The large triplet coupling arises (J(PH) = 75 Hz) from trans coupling of the bridging hydride with the two chemically equivalent phosphorus atoms P(2) and P(4). Similarly large PH coupling constants in related, spectroscopically characterized, binuclear rhodium phosphines with bridging hydrides have been observed previously.[16,63,64] All other ^{1}H and $^{31}P\{^1H\}$ spectral features are fully consistent with the solid-state structure.

Discussion

Clearly, from these results there is a large effect associated with changing the counterion from $[BF_4]^-$ to [*closo*-$CB_{11}H_{12}]^-$ or [*closo*-$CB_{11}H_6Br_6]^-$, the perhalogeno anion giving precatalysts that are significantly more active in alkene hydrogenation, which is on first inspection consistent with the coordinating ability of these anions.[17,38,65] The large difference observed between **4** (*closo*-$CB_{11}H_6Br_6$) and **A** (BF_4) is interesting, as on hydrogenation in CH_2Cl_2 both form complexes in which the anion does not interact with the metal[70] (i.e. complex **2**), unlike with **3**, where there exists a more intimate bond between metal center and carborane on initial hydrogenation (complex **1**). Whether these results suggest that the notionally least coordinating [*closo*-$CB_{11}H_6Br_6]^-$ counterion plays a significant role in the catalytic cycle, perhaps by stabilizing a reactive intermediate better than $[BF_4]^-$ does; or that, in contrast, the carborane simply does not interact with the metal center significantly compared with $[BF_4]^-$, resulting in faster turnover of the catalytic cycle, is not clear. The role of the counterion in olefin hydrogenation by cationic rhodium phosphine fragments partnered with sulfonate anions has recently been discussed, and it is suggested that the anion remains coordinated with the metal center throughout the catalytic cycle.[16] The proposed "low-pressure route" discussed in this particular system (ca. 1 atm of H_2) involves coordination of alkene first followed by oxidative addition of dihydrogen, with the sulfonate anion changing its denticity accordingly through the catalytic cycle. Significant counterion effects have also been reported in cationic iridium phosphanodihydrooxazole-based hydrogenation systems: moving from $[PF_6]^-$ to $[BAr_f]^-$ type counterions has a positive effect on conversion, enantiomeric excess, and catalyst stability in the high-pressure (50 bar) hydrogenation of sterically very-hindered stilbene derivatives, although the exact role of the counterion in the catalytic cycle remains unresolved.[15,66] In comparison, catalyst **4** effects essentially no conversion at room temperature and pressure of trans-α-methylstilbene to the corresponding alkane (<2% by GC after 6 h). This is probably due to the $\{(PPh_3)_2Rh\}^+$ fragment forming a catalytically inactive (at room temperature and pressure) η^6-arene complex with the stilbene precursor. In agreement with this observation, the toluene complex $[(PPh_3)_2Rh(\eta^6\text{-}C_6H_5Me)]$[*closo*-$CB_{11}H_6Br_6$] is a significantly poorer catalyst than **4** for the hydrogenation of cyclohexene, with only 10% conversion observed after 6 h under ambient conditions.

(61) Crabtree, R.; Parnell, C. A.; Uriate, R. J. *Organometallics* **1987**, *6*, 696.
(62) Crabtree, R.; Felkin, H.; Morris, G. E. *J. Organomet. Chem.* **1977**, *141*, 205.
(63) Butler, I. R.; Cullen, W. R.; Mann, B. E.; Nurse, C. R. *J. Organomet. Chem.* **1985**, *280*, C47.
(64) Morran, P. D.; Duckett, S. B.; Howe, P. R.; McGrady, J. E.; Colebrooke, S. A.; Eisenberg, R.; Partridge, M. G.; Lohman, J. A. B. *J. Chem. Soc., Dalton Trans.* **1999**, 3949.
(65) Patmore, N. J.; Hague, C.; Cotgreave, J.; Mahon, M. F.; Frost, C. G.; Weller, A. S. *Chem. Eur. J.* **2002**, *8*, 2088.
(66) Hou, D.-R.; Reibenspies, J.; Colacot, T.; Burgess, K. *Chem. Eur. J.* **2001**, *7*, 5391.

Conclusion

We have demonstrated that changing the counterion within the domain of *closo*-monocarboranes can have a significant effect on the efficiency of hydrogenation by cationic rhodium phosphine catalysts, to the extent that $[(PPh_3)_2Rh(nbd)][closo\text{-}CB_{11}H_6Br_6]$ will hydrogenate hindered alkenes, in reasonable yield, such as 2,3-dimethyl-2-butene, while $[(PPh_3)_2Rh(nbd)][closo\text{-}CB_{11}H_{12}]$ is essentially ineffectual, struggling to hydrogenate the less hindered methylcyclohexene. While this is not necessarily completely surprising, given the relative coordinating properties of these two carborane anions, it is satisfying to see that the system can be enhanced to significant effect by simply changing the carborane counterion. What is interesting is that $[BF_4]^-$ salts are significantly poorer than $[closo\text{-}CB_{11}H_6Br_6]^-$ salts for the hydrogenation of alkenes, especially when one considers that both anions do not interact significantly with the metal center on initial hydrogenation of the norbornadiene precursor. This perhaps implicates one of the following: (i) putative intermediate(s) in the catalytic cycle involve coordination of the counterion (which has precedent with other anions[13,16]), (ii) the $[BF_4]^-$ anion is somehow degraded in the catalytic cycle to form inactive metal fluorides or oxyborates, possibly activated toward this by coordination with the metal center, or (iii) a different mechanism operates with each of the two anions.

Overall this suggests that in Schrock−Osborn hydrogenation systems, as found with other systems where the cation/anion interaction is important such as metallocene olefin polymerization catalysts,[12] the match between anion and cation is a finely balanced one. The nature of the interaction between cation and anion is therefore of significant interest with regard to selecting the best combination and, thus, optimal performance. With regard to this we are currently considering the role of the carborane counterion in the catalytic cycle and anticipate reporting on this at a future date.

Experimental Section

All manipulations were carried out under an atmosphere of argon using standard Schlenk line techniques. Solvents were dried according to standard procedures and distilled under nitrogen. NMR solvents were dried over CaH_2 for at least 24 h, vacuum distilled, and freeze−pump−thawed prior to use. Cyclohexene, 1-methylcyclohexene, and 2,3-dimethyl-2-butene were passed through a column of activated alumina and freeze−pump−thawed prior to use. Gas chromatography was performed on a Perkin-Elmer Autosystem XL. NMR spectra were recorded on either a Bruker 300 MHz or a Varian 400 MHz spectrometer. ^{1}H NMR spectra were referenced using residual protio solvents, and ^{31}P NMR and ^{11}B NMR spectra were referenced to an external H_3PO_4 or $BF_3{\cdot}OEt_2$ reference, respectively. All NMR spectra were recorded at room temperature. Coupling constants are quoted in Hz. $[(PPh_3)_2RhCl]_2$,[47] $[(PPh_3)_2Rh(nbd)][BF_4]$,[49] $Ag[closo\text{-}CB_{11}H_{12}]$,[67] and $Ag[closo\text{-}CB_{11}H_6Br_6]$[68] were prepared by the reported literature routes. $[(py)(PCy_3)Ir(cod)][PF_6]$ was purchased from Aldrich and used as received.

$[(Ph_3P)_2Rh(closo\text{-}CB_{11}H_{12})]$ (1). $[(Ph_3P)_2RhCl]_2$ (0.212 g, 15.8 mmol) and $Ag[closo\text{-}CB_{11}H_{12}]$ (79 mg, 31.7 mmol) were dissolved in 5 mL of CH_2Cl_2, and the mixture was stirred for 3 h. The solution was filtered, and the CH_2Cl_2 solution was layered with hexane to afford **1** as red crystalline blocks (0.114 g, 47% yield). Anal. Calcd for for $C_{37}H_{42}B_{11}P_2Rh$: C, 57.68; H, 5.49. Found: C, 57.3; H, 5.25. ^{1}H NMR ($CDCl_3$): δ −1.97 (br q, J(BH) = 119, 1H, B*H*), −0.6−0.8 (broad q, J(BH) = 80.0, 5H, B*H*), 1.1−2.4 (br q, 5H B*H*), δ 2.6 (s, 1H CH_{cage}), 7.1−7.6 (m, 30H, C_6H_6). ^{1}H{^{11}B} NMR ($CDCl_3$): δ −1.97 (s, 1H, B$H_{antipodal}$), 0.1 (s, 5H, B*H*), δ 1.7 (s, 5H, B*H*), δ 2.6 (s, CH_{cage}), δ 7.1−7.6 (m, 30H, C_6H_6). ^{31}P{^{1}H} NMR: δ 49.0 (d, J(RhP) = 194 Hz). ^{11}B{^{1}H} NMR: δ −9.9 (1B), −13.5 (5B), −14.1 (5B).

$[(Ph_3P)(PPh_2\text{-}\eta^6\text{-}C_6H_5)Rh]_2[closo\text{-}CB_{11}H_6Br_6]_2$ (2). $[(Ph_3P)_2Rh(C_7H_8)][closo\text{-}CB_{11}H_{12}]$ (**4**; 25 mg, 0.0187 mmol) in 10 mL of CH_2Cl_2 was placed in a 100 mL Schlenk tube fitted with a new rubber septum. Via a needle, H_2 was bubbled through the solution for 10 min. The solution changed color from a golden orange to a claret red. The solvent was removed in vacuo. Crystals suitable for a single-crystal X-ray analysis were grown by slow diffusion of hexane into a CH_2Cl_2 solution of **2**. Yield: 0.021 g (90%). Anal. Calcd for $C_{74}H_{72}B_{22}Br_{12}P_4Rh_2{\cdot}1.4CH_2Cl_2$: C, 33.8; H, 2.9. Found: C, 34.1; H, 2.98. ^{1}H{^{11}B} NMR (CD_2Cl_2): δ 2.32 (s, 5H, B*H*), δ 2.54 (s, 1H, CH_{cage}), 5.32 (t, J(HH) = 6.6, 1H, C_6H_5), 6.58 (t, J(HH) = 6.6, 2H, C_6H_5), 6.97 (t, J(HH) = 6.6, 2H, C_6H_5), 7.0−7.25 (m, 20H, C_cH_5), 7.30 (t, J(HH) = 5.7, 4H, C_6H_5), 7.43 (t, J(HH) = 7.5, 4H, C_6H_5). ^{1}H NMR (CD_2Cl_2): δ 2.5−2.0 (br q, 5H, B*H*), 2.54 (s, 1H, CH_{cage}), 5.32 (t, J(HH) = 6.6, 1H, C_6H_5), 6.58 (t, J(HH) = 6.6, 2H, C_6H_5), 6.97 (t, J(HH) = 6.6, 2H, C_6H_5), 7.0−7.25 (m, 20H, C_cH_5), 7.30 (t, J(HH) = 5.7, 4H, C_6H_5), 7.43 (t, J(HH) = 7.5, 4H, C_6H_5). ^{31}P{^{1}H} (CD_2Cl_2): AA′BB′XX′ system, δ 47.5 (complex multiplet, J(RhP) = 216.6, J(RhP) = −0.2, J(PP) = 8.6), 44.6 (complex multiplet, J(RhP) = −1.0, J(Rh′P) = −199.3, J(PP) = 37.8, J(PP) = 1.32).

$[(Ph_3P)_2Rh(C_7H_8)][closo\text{-}CB_{11}H_{12}]$ (3). $(Ph_3P)_3RhCl$ (100 mg, 0.11 mmol), 2,5-norbornadiene (13 μL, 14 mmol), and $[Cs][closo\text{-}CB_{11}H_{12}]$ (30 mg, 0.11 mmol) were stirred in a 1:3 mixture of acetone and CH_2Cl_2 for 2 h. The resulting orange solution was filtered and concentrated in vacuo. The compound was crystallized by addition of ethanol. The solid was collected and washed with three portions of ethyl alcohol and dried in vacuo. Yield: 0.107 g (57%). Anal. Calcd for $C_{44}H_{50}B_{11}P_2Rh$: C, 61.26; H, 5.84. Found: C, 61.5; H, 5.85. ^{1}H NMR (CD_2Cl_2): δ 7.4−7.0 (m, 30H, C_6H_6), 4.5 (s, 4H, C_7H_8), 4.0 (s, 2H, C_7H_8), 2.7−1.0 (br q, 11H, B*H*), 2.35 (s br, 1H, CH_{cage}), 1.5 (s, 2H, C_7H_8). ^{31}P{^{1}H} NMR (CD_2Cl_2): δ 30.5 (d, J(RhP) = 154.5). ^{11}B{^{1}H} NMR (CD_2Cl_2): δ −4.0 (s, 1B), −10.3 (s, 5B), −13.1 (s, 5B).

$[(Ph_3P)_2Rh(C_7H_8)][closo\text{-}CB_{11}H_6Br_6]$ (4). $(Ph_3P)_3RhCl$ (100 mg, 0.11 mmol), 2,5-norbornadiene (13 μL, 14 mmol), and $[Cs][closo\text{-}CB_{11}H_6Br_6]$ (81 mg, 0.11 mmol) were stirred in a 1:3 mixture of acetone and CH_2Cl_2 for 2 h. The compound was isolated in the same manner as described for compound **3**. Yield: 0.162 g (60%). Anal. Calcd for $C_{46}H_{45}B_{11}Br_6P_2Rh$: C, 40.59; H, 3.33. Found: C, 40.4; H, 3.38. ^{1}H{^{11}B} NMR ($CDCl_3$): δ 7.4−7.0 (m, 30H, C_6H_6), 4.5 (s, 4H, C_7H_8), 4.0 (s, 2H, C_7H_8), 2.5 (s, 1H, CH_{cage}), 2.25 (s, 5H, B*H*), 1.5 (s, 2H, C_7H_8). ^{11}B{^{1}H} NMR ($CDCl_3$): δ 1.7 (s, 1B), −6.6 (s, 5B), −17.1 (s, 5B). ^{31}P{^{1}H} NMR ($CDCl_3$): δ 30.6 (J(RhP) = 155).

$[(Ph_3P)_2HRh(\mu\text{-}H)(\mu\text{-}Cl)_2RhH(PPh_3)_2][closo\text{-}CB_{11}H_{12}]$ (5). $[(Ph_3P)_2Rh(nbd)][closo\text{-}CB_{11}H_{12}]$ (25 mg, 0.03 mmol) in 10 mL of CH_2Cl_2 in a 100 mL Schlenk tube fitted with a rubber septum was pressurized with 20 psi of H_2 for 3 days. The solvent was concentrated in vacuo, and hexane (1 equal volume) was added via cannula. After refrigeration for 4−5 days the compound precipitated as yellow crystalline filaments suitable for a single-crystal X-ray analysis. This crystalline material contained ca. 5% of an unidentified product, which, in our hands, could not be removed by repeated recrystallization. Hence, accurate mass spectrometry on a bulk sample was used as an alternative to microanalysis. ^{1}H{^{11}B} NMR ($CDCl_3$): δ 7.3 (m, 60H, C_6H_6), 2.54 (s, 1H, CH_{cage}), 2.32 (s,

(67) Shelly, K.; Finster, D. C.; Lee, Y. J.; Scheidt, W. R.; Reed, C. A. *J. Am. Chem. Soc.* **1985**, *107*, 5955.
(68) Liston, D. J.; Lee, Y. J.; Scheidt, W. R.; Reed, C. A. *J. Am. Chem. Soc.* **1989**, *111*, 6643.

5H, B*H*), −11.0 (complex multiplet, 1H, part of a AA′BB′MXX′ system, Rh(*μ-H*), J(RhH) = 10, J(PH) = 21, 75), −16.5 (virtual quartet, 2H, J(RhP) = 15, J(PP) = 15, 15). $^{31}P\{^1H\}$ NMR ($CDCl_3$): δ 51.5 (complex m, AA′BB′XX′ system), 36.0 (complex m, AA′BB′XX′ system). Accurate mass spectrometry (ES+): calcd 1327.1367, found 1327.1353. Identical NMR spectra in the phosphine and hydride regions are obtained using $[CB_{11}H_6Br_6]$ as the counterion (i.e., starting from complex **4**).

General Procedure for Catalysis. In a Schlenk tube fitted with a new septum, the appropriate amount of catalyst was dissolved in CH_2Cl_2 (5 cm^3) to give a catalyst-to-substrate ratio of 1:100. The appropriate amount of alkene was added, and H_2 was bubbled (pressure 10 psi), via a needle, through the solution using an outlet needle for 10 min. The H_2 and outlet needles were then removed, and the reaction mixture was stirred for the appropriate amount of time, as indicated in Table 3. At this time a sample was prepared for gas chromatography by passing a portion (ca. 1 cm^3) of the solution through a short silica plug, washing the silica with CH_2Cl_2 (ca. 1 cm^3), and combining these two fractions.

X-ray Crystallography. The crystal structure data for compounds **1**, **2**, and **5** were collected on a Nonius KappaCCD, with pertinent details given in Table 1. Structure solution followed by full-matrix least-squares refinement was performed using the SHELX suite of programs throughout.[69,70] Plots were produced using ORTEX.[56]

Compound 2. Despite copious recrystallization efforts it did not prove possible to grow crystals of complex **2** with substantial dimensions for an X-ray structure determination. Thus, the crystal selected, while being the largest available from several batches, was extremely thin and of mediocre quality (mosaicity 1.56°). The smallest crystal dimension of 0.03 mm is reflected in the substantially larger than desirable R(int) and $R(\sigma)$ values (coupled with a not entirely satisfactory weighting scheme) than we normally obtain for data from our diffractometers. The electron density map of the asymmetric unit (half of a dimer molecule, proximate to a crystallographic inversion center) in this structure was also seen to contain two areas pertaining to solvent. The first of these was modeled as one whole molecule of dichloromethane with the two chlorines therein refined over four positions, each at half-occupancy. The second solvent area was more diffuse, and several models were tried. The best convergence was achieved by refining this area as 0.39 of a dichloromethane molecule with the two associated chlorines equally disordered over three sites. Hydrogen atoms were omitted from the refinement in the solvent areas due to the disorder. One of the phenyl rings in the rhodium dimer also exhibited disorder, which was successfully modeled at 65:35 occupancy for C(32)−C(37) and C(32)′−C(37)′, respectively. Trial runs of applying an absorption correction to the data for this structure afforded no improvement in convergence, and hence, this correction type was omitted.

Compound 5. As with **2**, numerous efforts at recrystallization proved unsuccessful in growing crystals with substantial dimensions for an X-ray structure determination for complex **5**. The crystal selected, while being the best available, was extremely thin and of very poor quality. As with **2**, the smallest crystal dimension (0.05 mm) is reflected in the larger than desirable R(int) and $R(\sigma)$ values and poorer R factors than we would normally obtain from our diffractometers. Nevertheless, the structure converged well and, surprisingly, the reliable location of the hydrogens attached to the rhodium centers was possible. These particular hydrogens were positionally refined subject to constraints in the final least-squares analysis. The asymmetric unit in this structure was also seen to contain one molecule of dichloromethane, disordered over 2 sites in a 50:50 ratio. Trial runs of applying an absorption correction to the data for this structure afforded no improvement in convergence and, hence, were abandoned in the final least-squares cycles.

Acknowledgment. A.S.W. thanks the Royal Society for a University Research Fellowship and equipment grant (GC). The EPSRC and the University of Bath are also thanked for financial support (studentships to A.R. and N.J.P., respectively). The use of the Cambridge Structural Database at Daresbury service is acknowledged. The EPSRC/JREI is acknowledged for funding for a Nonius Kappa-CCD diffractometer, while use of the EPSRC mass spectrometry service at the University of Swansea is also acknowledged. Johnson Matthey PLC is thanked for the loan of platinum group metal salts.

Supporting Information Available: Tables giving crystallographic data and structure refinement details, positional and thermal parameters, and bond distances and angles for complexes **1**, **2**, and (**5**)$[CB_{11}H_{12}]$ (these data are also available as CIF files) and figures giving calculated and experimental $^{31}P\{^1H\}$ NMR spectra for complexes **2** and $[\mathbf{5}]^+$. This material is available free of charge via the Internet at http://pubs.acs.org.

OM020077R

(69) Sheldrick, G. M. SHELX-97: A Computer Program for Refinement of Crystal Structures; University of Göttingen, Göttingen, Germany.

(70) A CH_2Cl_2 solution $[(PPh_3)_2Rh(nbd)][BF_4]$ was treated with H_2 for 10 min, the volatiles were removed in vacuo, and the residue was taken up in CD_2Cl_2. ^1H NMR and $^{31}P\{^1H\}$ NMR spectroscopy indicated the formation of an arene-briged dimer complex, similar to **2**.